Effect of La_2O_3 addition on Ni/Al_2O_3 catalysts to produce H_2 from glycerol

N.D. Charisiou[1], G. Siakavelas[1], K.N. Papageridis[1,2], M.A. Goula[1,2]

[1]Department of Environmental and Pollution Control Engineering, Technological Educational Institute of Western Macedonia (TEIWM), GR – 50100, Koila, Kozani, Greece
[2]Catalysis and Environmental Protection MSc, School of Science and Technology, Hellenic Open University, Parodos Aristotelous 18, GR - 26335, Patras, Greece

ABSTRACT

Biodiesel has been promoted as the only realistic alternative to petro-oil in the transport sector, as it can be mixed in any ratio with standard diesel for use in diesel engines. However, the increase in biodiesel production has been accompanied by increases in glycerol production, which is the main by-product of the process. As hydrogen is a clean energy carrier, conversion of glycerol to hydrogen is one among the most attractive ways to make use of this byproduct.

In this study, the catalytic production of hydrogen by steam reforming of glycerol has been experimentally performed in a fixed-bed reactor. The performance of this process was evaluated over nickel (Ni) supported on un-promoted and promoted with La_2O_3 alumina catalysts. Catalysts were synthesized applying the wet impregnation method at a constant metal loading (8wt%). The synthesized samples, at their calcined or/and reduced form, were characterized by X-Ray Diffraction (XRD) and the N_2 adsorption-desorption technique (BET). Their chemical composition was determined by inductively coupled plasma (ICP), while the deposited carbon on the catalytic surface was measured by a CHN analyzer. Morphological examination and elemental analysis was done using Scanning Electron Microscopy (SEM) and Energy Dispersive Spectroscopy (EDS) respectively, for both fresh and used catalysts. The catalytic performance of the catalysts concerning the glycerol steam reforming reaction was studied in order to investigate the effect of the reaction temperature on (i) Glycerol total conversion, (ii) Glycerol conversion to gaseous products, (iii) Hydrogen selectivity and yield, (iv) Selectivity of gaseous products, and (v) Selectivity of liquid products.

From the work presented herein, it can be concluded that the addition of lanthanum to Ni catalysts supported on alumina favors the formation of gaseous H_2 and CO_2, minimizes liquid effluents and inhibits the formation of carbon during the reaction. The fall in carbon formation may be attributed to the lanthanum's redox properties, which offer alternative routes to the removal of carbon.

Keywords: biodiesel, glycerol, hydrogen, steam reforming, nickel supported catalysts

1. INTRODUCTION

Arguably, fossil based energy has been the prime mover for the unprecedented socio-economic development that the world has experienced since the industrial revolution. However, in the past decades, the limited nature of these resources, issues of accessibility and affordability, the emergence of China and India as major fossil fuel consumers, as well as the anxiety that has been caused by the possible effects of climate change, have provided a fresh impetus in the quest for alternative energy sources (Mathews, 2014; Winzer, 2012). Among the various Renewable Energy Systems (RES) that have been developed, the use of biomass as potential energy provider has gained considerable attention, especially in the field of biofuels, as the only realistic alternative to petro-oil (Abou-Shanab, et. al., 2014; Panepinto, et. al., 2014). As a result, global biofuel production has been increasing rapidly over the last decade, but the expanding biofuel industry has recently raised important concerns. In particular, the sustainability of many first - generation biofuels (which are produced primarily from food crops such as grains, sugar cane and vegetable oils) has been increasingly questioned over concerns such as reported displacement of food-crops, effects on the environment and climate change (Manivannan and Narendhirakannan, 2015; Marx and Venter, 2014).

Biodiesel is chemically non-toxic in nature, biodegradable, has insignificant contribution to CO_2 and other particulate matter emissions, it can be employed directly in conventional petroleum-diesel engines giving optimal performance, particularly due to very low sulfur and aromatic contents and compatible flash, cloud and pour points (Prakash, et. al., 2013). Biodiesel is currently produced from the transesterification reaction between vegetable oils or animal fats (mainly, sunflower, rapeseed oils, palm oil, canola oil, cotton seed, soybean, Jatropha curcas, algae, waste frying oils, non-edible oils) and principally methanol (although ethanol is also used to a lesser extent) in the presence of an acidic or alkaline catalyst to form the biodiesel; fatty acid methyl esters (FAME) or fatty acid ethyl esters (Atadashi, 2013; Ngamlerdpokin, et. al., 2011; Passel, et. al., 2013; Pitakpoolsil and Hunsom, 2014). The process is described schematically in Figure 1. One of the barriers for the further development and commersialization of biodiesel is its high production cost, which is caused by the price of raw materials (Atapour and Kariminia, 2013; Nuchdang and Phalakornkule, 2012). Thus the industry needs to find new and innovative ways of maximizing its profits either by bringing down the cost of raw materials (hence the move towards making use of waste cooking oils) and/or by making use of its existing waste streams.

Figure 1. Transesterification process (Chavalparit and Ongwandee, 2009)

The principal byproduct of the biodiesel industry is glycerol, as every 100g of oil undergoing the transesterification process produces 10g of glycerol as byproduct. The glycerol so obtained is crude as it contains nonreacted and partially reacted fats, free fatty acids, methanol, esters and salts, and thus, it cannot be used as raw material in the pharmaceutical and cosmetic industries (Khanna, et. al., 2014). A viable solution could be the reconstruction of biodiesel plants into novel biorefineries through the integration of glycerol-based bioconversions in existing lines for the production of various chemicals (Kachrimanidou, et. al., 2013) or the production of synthesis gas and hydrogen (Escribà, et. al., 2013). However, the steam reforming of glycerol involves complex reactions that result in several intermediates, affecting the selectivity of the hydrogen. Moreover, the most important difficulty presented by the process is the high carbon formation rate (Iriondo, et. al., 2009; Wu, et al., 2014). The formation route of synthesis gas (CO and H_2), a highly endothermic reaction that favors high temperatures, may be observed in Figure 2 (Bobadilla et. al., 2014).

Figure 2. Scheme of reactions involved in the steam reforming of glycerol. Values not in parentheses correspond to ΔH at 250°C, and values within parentheses correspond to ΔG° at 250°C

Monometallic supported catalysts based on Ni, Pd, Pt, Ru, Rh and Ir have been studied in the steam reforming of glycerol, with a number of studies showing that Ni supported catalysts exhibit good reforming activity (Adhikari, et., al., 2007a; Bobadilla, et. al., 2014; Buffoni, et. al., 2009; Iriodo, et. al., 2009). Among supports, alumina-based supports are often used in reforming catalysts because of their mechanical and chemical resistance under reaction conditions. Nevertheless the use of alumina as support promotes catalysts deactivation by deposition of carbon. Thus, basic additives or promoters that favor water adsorption and OH surface mobility are usual in Al_2O_3 supports to neutralize its acidity and to decrease the rate of coke deposition on catalysts surfaces (Sánchez-Sánchez, et. al., 2007). Alternatively, coking may be reduced by gasifying the deposited carbon species something that can be achieved by adding lanthanide oxides on the support (Meeyoo, et. al., 1998; Tsipouriani, et. al., 1998).

In this contribution a comparative study of catalytic performance for nickel (Ni) supported on un-promoted and promoted with La_2O_3 alumina catalysts is reported. Catalysts were synthesized applying the wet impregnation method at a constant metal loading (8wt%). The synthesized samples, at their calcined or/and reduced form, were characterized by X-Ray Diffraction (XRD) and N_2 adsorption-desorption technique (BET). The chemical composition of the catalysts was determined by inductively coupled plasma (ICP), while the deposited carbon on the catalytic surface was measured by an CHN analyzer. Morphological examination and elemental analysis was done using Scanning Electron Microscopy (SEM) and Energy Dispersive Spectroscopy (EDS) respectively, for both fresh and used catalysts. The catalytic performance of the catalysts concerning the glycerol steam reforming reaction was studied in order to investigate the effect of the reaction temperature on (i) Glycerol total conversion, (ii) Glycerol conversion to gaseous products, (iii) Hydrogen selectivity and yield, (iv) Selectivity of gaseous products, and (v) Selectivity of liquid products.

2. MATERIALS AND METHODS

2.1 Catalysts Preparation
The alumina support was purchased in pellet form from Akzo, while the lanthanum-alumina (containing 4 wt. % La_2O_3) was obtained from W. R. Grace (MI-386) in powder form. The physicochemical properties of the γ-alumina and lanthanum-alumina used in this study are presented in Table 1. The γ-Al_2O_3 support was crashed and sieved to 350-500μm, while the LaAl support was first pelletized and then crashed and sieved to the same size. The as prepared supports where calcinated at 800 ^{o}C for 4 h. The catalysts were prepared via the wet impregnation technique using $Ni(NO_3)_2$ $6H_2O$ aqueous solutions with the proper concentration, in order to obtain final catalysts with Ni content of about 8 wt%. The nickel nitrate for the catalyst preparation was obtained from Sigma Aldrich. All solutions for catalyst preparation throughout this study utilized distilled and deionised pure water generated by NANOpure Diamond UV unit (Barnstead International). The resulting slurries were evaporated using a rotary evaporator at 75 ^{o}C for 5 h and dried at 120 ^{o}C for 12 h followed by calcination at 800 ^{o}C for 4 h. The samples were labeled as Ni/Al and Ni/LaAl.

Table 1. Physicochemical properties of the γ-alumina and lanthanum-alumina used in the study

Property	Al	LaAl
Radius (R)	1.58×10^{-3} m	n/a
Mean pore diameter (α)	7.8×10^{-9} m	n/a
Surface area (S_{BET})	281 m^2g^{-1}	176 m^2g^{-1}
Bed density (ρ_B)	5.7×10^5 g m^{-3}	n/a
Pore volume (V_p)	0.65 ml g^{-1}	0.77 ml g^{-1}
Average length (L)	5.2 mm	n/a

Note: n/a = not available

2.2 Catalysts Characterization
BET surface areas (SBET) of the catalytic samples were determined by the N_2 adsorption–desorption isotherms at -196°C using the Nova 2200e (Quantachrome) flow apparatus, according to Brunauer-Emmett-Teller (BET) method at the relative pressure in the range of 0.05–0.30. The total pore volume calculation was based on nitrogen volume at the highest relative pressure, whereas the average pore size diameter was determined by the Barrett-Joyner-Halenda (BJH) method. Prior to the measurements the samples were degassed at

350°C for 5 h under vacuum. The total metal loading (wt%) of the final catalysts' was determined by the Inductively Coupled Plasma Atomic Emission Spectroscopy (ICP-AES) on a Perkin-Elmer Optima 4300DV apparatus. The catalysts' crystalline structure was determined by applying the X-ray diffraction (XRD) technique, using a ThermoAl diffractometer with Cu-Ka radiation. The diffraction pattern was identified by comparison with those of known structure in the JCPDS (Joint Committee of Powder Diffraction Standards) database. It should be noted that the XRD technique was used for both fresh and reduced samples. The Scherrer equation, if applicable, was employed to determine the particle size of different phases based on their most intense diffraction peaks. Morphological examination of both fresh and used catalysts was done using Scanning Electron Microscopy (SEM) in a JEOL 6610LV. The elemental analysis, by means of Energy Dispersive Spectroscopy (EDS), was carried out using a large area (80mm^2) silicon drift detector (X-Max 80 Oxford Instruments). Images, elements maps and spectra were acquired and analyzed with the AZtech Nanoanalysis software (Oxford Instruments). The percentile concentration of carbon in the used catalysts was determined by a Leco CS-200 analyser, using 0.1 g of each sample.

2.3 Catalytic performance

The glycerol steam reforming reaction was carried out at atmospheric pressure, in a continuous flow, fixed-bed, single pass, tubular stainless steel reactor, with an inner diameter of 14 mm, at temperature ranging from 400-750°C (Figure 3). The experimental set up used allowed the feeding of both liquid and gaseous streams, having two vaporizers and a pre-heater before the reactor and a condenser after it. The vaporizers, pre-heater and reactor are placed into electrical ovens and regulated with programmed-temperature controllers.
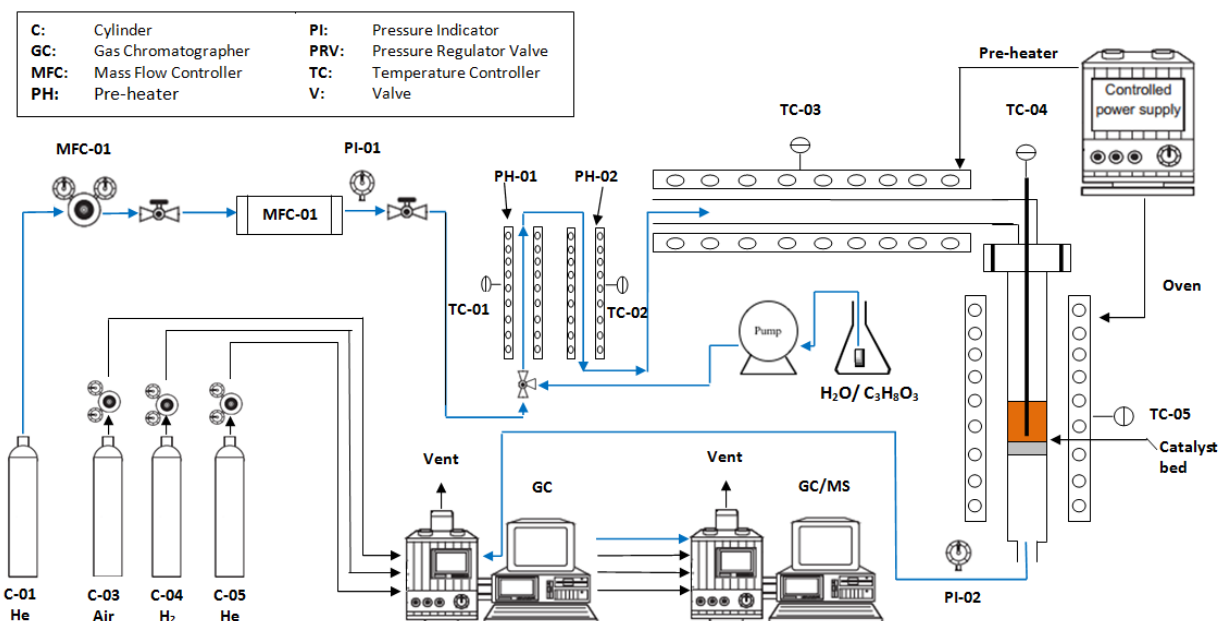
Figure 3. Schematic flow chart of experimental setup for activity test of catalysts towards glycerol steam reforming

The liquid stream consisted of $C_3H_8O_3$ (20% w.w.) and H_2O (total liquid flow rate = 0.12 ml/min). The glycerol used had 99.5% purity and was obtained from Sigma Aldrich. The glycerol/ water mixture was fed with a HPLC pump (Series I) and was first vaporized at 350°C before it was mixed with He (He flow rate = 38 ml/min). The reactor's outlet gases passed

through a cold trap for liquid products capture. Prior to catalytic testing, 200 mg of catalyst sieved to 350-500 μm was reduced in situ in a hydrogen flow (100 ml/min) at 800°C for 1 hr. The gaseous products were analyzed on-line by a gas chromatographer (Agilent 7890A), with two columns in parallel, HP-Plot-Q (19095-Q04, 30 m length, 0.530 mm I.D.) and HP-Molesieve (19095P-MSO, 30 m length, 0.530 mm I.D.), equipped with TCD and FID detectors. Liquid products were analyzed via a combination of Gas Chromatography (Agilent 7890A, with a 5MS column, equipped with an FID detector) and Mass Spectroscopy (Agilent 5975C).

The performance of the catalysts in the gas phase is reported in terms of H$_2$ yield, H$_2$, CO, CH$_4$ and CO$_2$ selectivity, glycerol conversion into gaseous products, and total glycerol conversion. Moreover, the performance of the catalysts in the liquid phase is reported in terms of acetol (C$_3$H$_6$O$_2$), acetone [(CH$_3$)$_2$CO], allyl alcohol (CH$_2$=CHCH$_2$OH), acetaldehyde (C$_2$H$_4$O) and acetic acid (C$_2$H$_4$O) selectivity. Performance parameters were calculated based on the following equations:

$$\% Glycerol\ conversion = \left[\frac{(Glycerol\ in) - (Glycerol\ out)}{Glycerol\ in} \right] \times 100 \tag{1}$$

$$\% Glycerol\ conversion\ into\ gaseous\ products = \frac{C\ atoms\ in\ gas\ products}{Total\ C\ atoms\ in\ the\ feedstock} \times 100 \tag{2}$$

$$H_2\ Yield = \frac{H_2\ moles\ produced}{moles\ of\ glycerol\ fed} \tag{3}$$

$$\% H_2\ Selectivity = \frac{H_2\ moles\ produced}{C\ atoms\ produced\ in\ gas\ phase} \times \frac{1}{RR} \times 100 \tag{4}$$

where, RR is the reforming ratio (7/3), defined as the ratio of moles of H$_2$ to CO$_2$ formed.

$$\% Selectivity\ of\ i = \frac{C\ atoms\ in\ spieces\ i}{C\ atoms\ produced\ in\ gas\ phase} \times 100 \tag{5}$$

where, species i refers to CO, CO$_2$ and CH$_4$.

$$\% Selectivity\ of\ i' = \frac{C\ atoms\ in\ spieces\ i'}{C\ atoms\ produced\ in\ liquid\ phase} \times 100 \tag{6}$$

where, species i' refers to acetol, acetone, allyl alcohol, acetaldehyde and acetic acid.

3. RESULTS AND DISCUSSION

3.1 Characterisation results

In Table 2 the physicochemical properties of all samples are presented. As can be observed, the specific surface area (SSA, i.e., S$_{BET}$) for the supported nickel on Al$_2$O$_3$ catalyst is significantly lower than the one of the supporting material (γ-Al$_2$O$_3$, 195 m^2 g^{-1}, after calcination at 800°C), whereas the pore volume (Vp) was not significantly altered. The lower surface area can be attributed to the fact that the internal surface area of the support pore system is probably progressively covered by nickel species adsorbed on alumina active sites forming a layer (Bereketidou and Goula, 2012). These results are nearly identical to those obtained by Cheng, et. al., (2011) for a similar Ni/Al catalyst system. It should also be noted that both catalyst

samples (Ni/Al and Ni/LaAl) have comparable SSA's. The ICP results (metal loading) indicate that the desired metal level was achieved for both catalysts.

Figure 4 and 5 depict the XRD patterns of the Ni/Al and Ni/LaAl catalyst after calcination and after reduction. Characteristic peaks at $2\theta= 35.2^o$, 47.2^o and 67.6^o (for the Ni/Al), and $2\theta= 35.1^o$, 47.1^o, 60.02^o and 67.4^o (for the Ni/LaAl) assigned to poorly crystaline γ-Al_2O_3 and peaks of the spinel nickel aluminate phase ($NiAl_2O_4$), indicated by the intensity of diffraction lines at $2\theta=19^o$, 32°, 37°, 60.2^o and 65.9^o can be observed for both samples. It should be noted that an additional peak at $2\theta=45^o$ is observed for the Ni/Al catalyst which can be attributed to either $NiAl_2O_4$ or NiO (Cheng, et. al., 2011). The formation of $NiAl_2O_4$ is caused by the reaction of NiO and Al_2O_3 due to the high calcination temperature, i.e., T=800°C (Coo et. al., 2014; Dou, et. al., 2014). The appearance of two small peaks at $2\theta=44^o$ and 51.2^o on the reduced samples indicate the presence of metallic Ni^o (Franchini, et. al., 2014). On the other hand, no diffraction peaks of the La_2O_3 phase were detected in either the calcinated or reduced Ni/LaAl samples (Figure 5), indicating either an amorphous structure or that it is highly dispersed in the γ-Al_2O_3 (Garbarino, et. al., 2015; Melchor-Hernández, et. al., 2013).

Table 2. Characterization results of the calcined, reduced and used catalysts

Catalyst/ Support	S_{BET} (m^2g^{-1})	V_p $(ml\ g^{-1})$	Metal loading (Ni, wt%)	Carbon (%)
Al (c)	195	0.65	-	-
LaAl (c)	n/a	0.70	-	-
8Ni/Al (c)	158	0.58	7.14	-
8Ni/Al (r)	-	-	-	-
8Ni/LaAl (c)	159	n/a	7.79	-
8Ni/LaAl (r)	-	-	-	-
8Ni/Al (u)	-	-	-	34.35
8Ni/LaAl (u)	-	-	-	18.04

Note: c = calcinated, r = reduced, u = used, n/a = not available
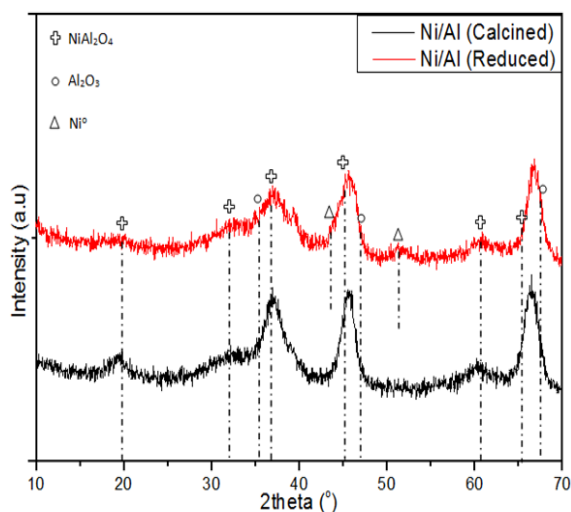
Figure 4. XRD patterns of calcined and reduced (at 800°C) Ni/Al catalysts
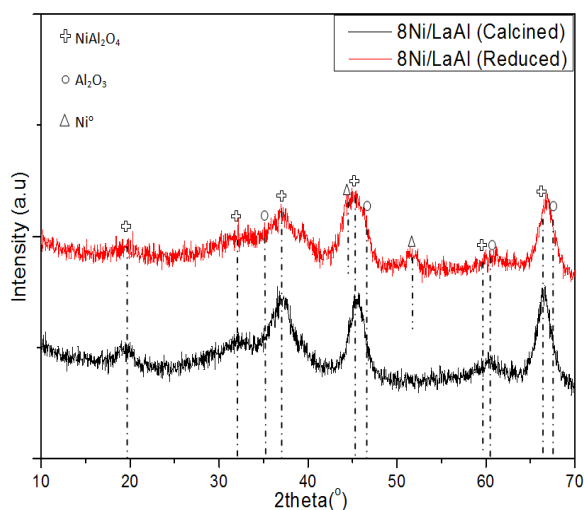
Figure 5. XRD patterns of calcined and reduced (at 800°C) Ni/LaAl catalysts

Figure 6 shows the SEM images of the Ni/Al catalyst before use (fresh) at different magnifications (x400 for image (a), and x2700 for image (b)). As can be observed the catalyst is of non uniform morphology and includes large ensembles, as well as, micro and nano particles. EDS Ni measurements are in agreement with the ICP results presented on table 2, showing a metal loading of 7.3%. The presence of carbon deposits over the catalyst used in the reaction was also examined be SEM. Figure 7(a) reveals a picture that shows that the catalyst has undergone significant transformation in its morphology; plane particles and others with rugged appearance are shown. When carbon quantification is performed it reveals that in the Ni/Al catalyst, carbon is concentrated on specific areas (Fig 7b), most probably those where metallic Ni^o is to be found, leading to the catalyst's quicker deactivation. This was also confirmed in the EDS spectra which showed that only 4.0% of the Ni could be identified.
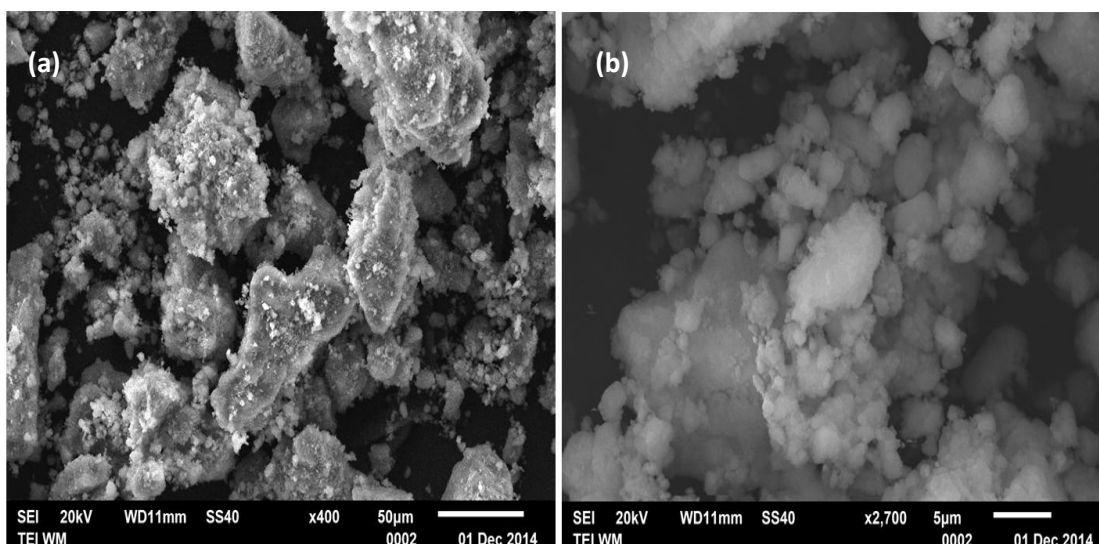
Figure 6. SEM images of the fresh Ni/Al catalyst
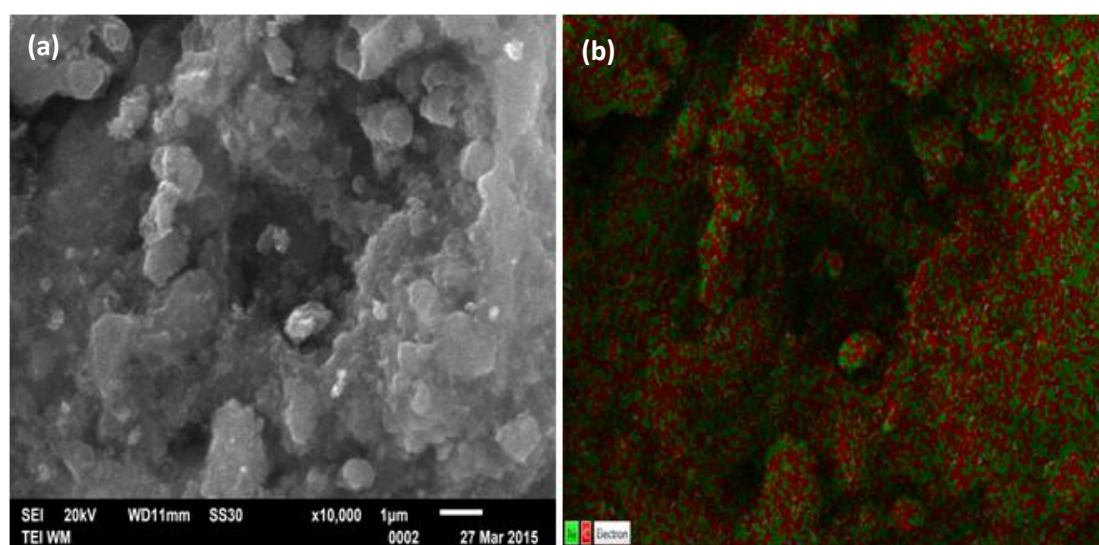
Figure 7. (a) SEM images of the used Ni/Al catalyst, (b) Carbon mapping of the used Ni/Al catalyst

3.2. Catalytic activity and selectivity

Thermodynamic studies predict that high temperatures, low pressures and high H_2O/C ratio favor hydrogen production. A number of researchers suggest that the ideal condition to obtain hydrogen is at reaction temperatures higher than $627^{\circ}C$ with a molar ratio of water to glycerol higher than 9. Under these conditions, methane production is minimized and carbon formation is thermodynamically inhibited. Although excess water allows higher selectivity to hydrogen, a significant water amount in reaction products is not beneficial (Adhikari, et al., 2007b; Buffoni, et. al., 2009). Thus, in this work, reaction tests were carried out in a temperature range of 400-$750^{\circ}C$, at atmospheric pressure and for a water-glycerol molar ratio of 20:1.

Glycerol total conversion (global conversion) and glycerol conversion into gaseous products is presented in Fig. 8. As can be clearly observed, both catalysts show improvements with increased temperatures (a consequence of the endothermic nature of the overall steam reforming reaction) however, the Ni/LaAl catalyst exhibits significantly higher conversions into gaseous products. The difference is particularly marked between 500-$600^{\circ}C$, where the Ni/LaAl catalysts conversion is ~60-80%, as opposed to ~40-60% for the Ni/Al catalyst.
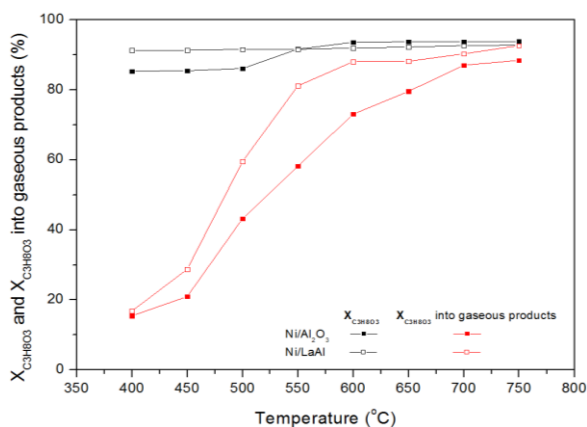
Figure 8. Total glycerol conversion and glycerol conversion into gaseous products
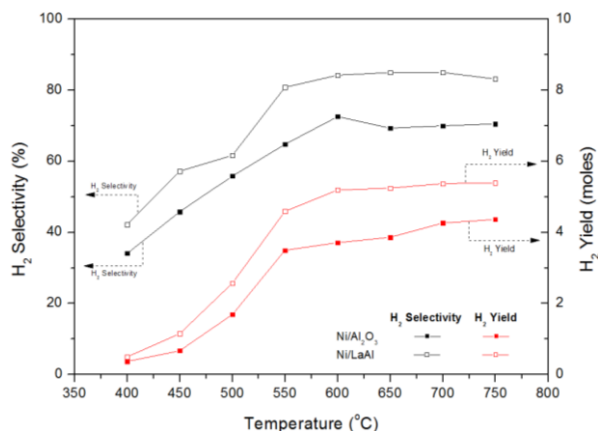
Figure 9. Hydrogen yield and selectivity
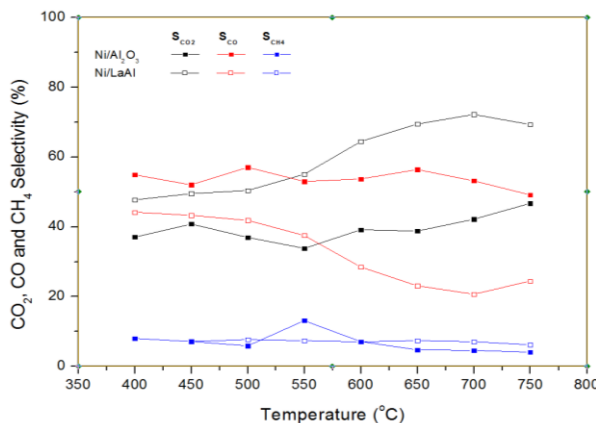
Figure 10. CO_2, CO and CH_4 selectivity (%)

GC analysis revealed that the gaseous products were H_2, CO_2, CO and CH_4. Previous work by other researchers also indicated that these gases are the main products of glycerol steam reforming (Siew, et. al., 2014; Zhang, et. al., 2007). Hydrogen yield and selectivity (%) are presented in Fig. 9, while CO_2, CO and CH_4 selectivity (%) are presented in Fig. 10. For both

catalysts, the formation of CH_4 is considerably low during the whole temperature range. There are two main reactions which can take place in high temperatures with a steam/glycerol mixture: steam reforming and decomposition. The reactions occur simultaneously in the fixed-bed reactor including H_2 production and other side reactions (Cheng, et. al., 2011; Pompeo, et. al., 2011). The concentration of H_2 produced from glycerol steam reforming and decomposition increases with increasing temperatures for both catalysts (Figure 9). Again for the Ni/LaAl catalyst, hydrogen yield and hydrogen selectivity is significantly enhanced (Fig. 9) for the entire temperature range, while interestingly, the production of CO_2 (selectivity) increases with temperature, while that of CO decreases (Fig. 10). The opposite is true for the Ni/Al catalyst, i.e., the production of CO_2 (selectivity) decreases with temperature, while that of CO increases. This is significant as the presence of CO in the gas mixture can adversely affect the performance of both anode and cathode in proton-exchange fuel cells (PEMFCs) acting as poison (Chen, et. al., 2013; Qi, et. al., 2002).

Condensed reaction products (liquid products) presented a yellowish colour and by combined gas chromatography and mass spectroscopy CG/MS a number of compounds were identified and quantified. These compounds, identified for both catalysts, were acetic acid, acetaldehyde, allyl alcohol, acetone and acetol (Table 3). The liquid effluents identified herein are in broad agreement with work by previous researchers (Buffoni, et. al., 2009; Dou, et. al., 2014; Thyssen, et. al., 2013). These products where present mainly at relatively low temperature ranges, which can be attributed to the different reaction routes that convert glycerol to liquid products (e.g. glycerol hydrogenolysis) that are exothermic in character (Franchini, et. al., 2014). Indeed the values accomplished for the catalysts presented herein are in good agreement with those presented by other researchers (Cheng, et, al., 2011). However, significant differences were observed between the two catalysts. Specifically, for the Ni/Al catalyst, the reaction compounds were produced from 400-650°C, with acetone's selectivity reaching ~70% (at 650°C) and acetol's selectivity ~40% at 600°C (Table 3). Thus, the Ni/Al catalyst exhibits high glycerol conversion into liquid products (and hence, low glycerol conversion into gaseous products) for the temperature range of 400-650°C. Again, the opposite is true for the Ni/LaAl catalyst, which seems to produce liquid products only up to 550°C, with acetol (~43% at 500°C) and acetone (~35% at 550°C) as the main by-products (Table 3).

Table 3. Liquid products' selectivity for the Ni/Al and Ni/LaAl catalyst

Ni/Al							
Compounds	**Reaction temperature ($^{\circ}$C)**						
	400	**450**	**500**	**550**	**600**	**650**	**700**
Acetol	33.75	40.45	44.92	38.23	2.10	0.00	0.00
Acetone	20.75	23.02	20.76	24.49	42.19	70.16	0.00
Allyl alcohol	14.20	14.02	12.42	13.84	23.26	10.82	0.00
Acetaldehyde	21.56	13.99	12.25	13.23	18.15	19.02	0.00
Acetic acid	9.75	8.53	9.65	10.21	14.31	0.00	0.00
Ni/LaAl							
Acetol	31.33	42.48	43.03	0.72	0.00	0.00	0.00
Acetone	17.97	18.42	20.02	35.67	0.00	0.00	0.00
Allyl alcohol	24.98	17.09	13.77	21.88	0.00	0.00	0.00
Acetaldehyde	17.97	13.23	14.34	25.55	0.00	0.00	0.00
Acetic acid	7.75	8.79	8.84	16.18	0.00	0.00	0.00

Unfortunately, studies on carbon deposition over Ni-based catalysts and the mechanism of coke formation for the steam reforming of glycerol are still missing in the literature. However, some contributions have reported the deactivation of Ni-supported catalysts on SR of Glycerol and associated this phenomenon with the formation of both highly reactive carbon species and low reactive, more ordered structures, particularly filamentous carbon (Buffoni, et. al., 2009; Cheng, et, al., 2011; Dieuzeide, et. al., 2013; Franchini, et. al., 2014; Siew, et. al., 2014). Thus, the better performance of the Ni/LaAl catalyst can be probably attributed to the inclusion of lanthanum, which has increased the basicity of the catalyst and reduced carbon formation (Siew, et. al., 2014). It has also been suggested that the multiple oxidation states exhibited by lanthanide elements provide an additional route for conversion of carbonaceous species during reforming via redox reactions (Foo, et. al., 2012). This reduction in carbon formation was also confirmed by our measurements in a Leco CS-200 analyser, which reveal that the percentage of carbon formed on the Ni/LaAl catalyst was almost half of that formed on the Ni/Al catalysts, i.e., 18.04% and 34.35% respectively (Table 2). The use of additional analytical techniques, such as Transmission Electron Microscopy (TEM) and Temperature-Programmed Oxidation (TPO), on post reaction samples, will help us identify the nature of the carbonaceous species deposited on the catalysts, and perhaps, allow us to contribute to the discussion of defining the pathway of catalyst deactivation.

4. CONCLUSIONS

The need to move from fossil based resources to renewable energy systems has led to the promotion of biodiesel as the only realistic alternative to petro-oil in the transport sector. However, the increase in biodiesel production has been accompanied by increases in glycerol production, which is the main by-product of the process. Glycerol valorization to hydrogen or syngas is one of the prospective ways to alleviate our dependence on fossil fuels and mitigate this waste management issue. Heterogeneous catalysis plays a critical role in converting glycerol to hydrogen and syngas. The addition of promoters to a catalyst's support can improve selectivity and durability, mitigating typical problems with catalysts that include coke formation, active oxidation, sintering, and segregation.

From the work presented herein, it can be concluded that the addition of lanthanum to Ni catalysts supported on alumina favors the formation of gaseous H_2 and CO_2, minimizes liquid effluents and inhibits the formation of carbon during the reaction. The fall in carbon formation may be attributed to the lanthanum's redox properties, which offer alternative routes to the removal of carbon.

REFERENCES

Abou-Shanab, R.A.I., Ji, M.K., Kim, H.C., Paeng, K.J., Jeon, B.H., 2013. Microalgal species growing on piggery wastewater as a valuable candidate for nutrient removal and biodiesel production. Journal of Environmental Management, 115, 257-264.

Adhikari, S., Fernando, S., Haryanto, A., 2007a. Production of hydrogen by steam reforming of glycerin over alumina-supported metal catalysts. Catalysis Today, 129, 355-364.

Adhikari, S., Fernando, S., Gwaltney, S.R., To, S.D.F., Bricka, R.M., Steele, P.H., Haryanto, H., 2007b. A thermodynamic analysis of hydrogen production by steam reforming of glycerol. International Journal of Hydrogen Energy, 32, 2875-2880.

Atadashi, I.M., Aroua, M.K., Abdul Aziz, A.R., Sulaiman, N.M.N., 2013. The effects of catalysts in biodiesel production: A review. Journal of Industrial and Engineering Chemistry, 19, 14-26.

Atapour, M., Kariminia, H.R., 2013. Optimization of biodiesel production from Iranian bitter almond oil using statistical approach. Waste and Biomass Valorization, 4(3), 467-474.

Bereketidou, O.A., Goula, M.A., 2012. Biogas reforming for syngas production over nickel supported on ceria-alumina catalysts. Catalysis Today 195, 93-100.

Bobadilla, L.F., Penkova, A., Romero-Sarria, F., Centeno, M.A., Odriozola, J.A., 2014. Influence of the acid-base properties over NiSn/MgO-Al$_2$O$_3$ catalysts in the hydrogen production from glycerol steam reforming. International Journal of Hydrogen Energy, 39, 5704-5712.

Buffoni, I.N., Pompeo, F., Santori, G.F., Nichio, N.N., 2009. Nickel catalysts applied in steam reforming of glycerol for hydrogen production. Catalysis Communications, 10, 1656-1660.

Chavalparit, O., Ongwandee, M., 2009. Optimizing electrocoagulation process for the treatment of biodiesel wastewater using response surface methodology. Journal of Environmental Science 21(11), 1491–1496.

Chen, C.Y., Lai, W.H., Yan, W.M., Chen, C.C., Hsu, S.W., 2013. Effects of nitrogen and carbon monoxide concentrations on performance of proton exchange membrane fuel cells with Pt–Ru anodic catalyst. Journal of Power Sources, 243, 138-146.

Cheng, C.K. Foo, S.Y., Adesina, A.A., 2011. Steam reforming of glycerol over Ni/Al$_2$O$_3$ catalyst. Catalysis Today, 178, 25-33.

Dieuzeide, M.L., Jobbagy, M., Amadeo, N., 2013. Glycerol steam reforming over Ni/γ-Al$_2$O$_3$ catalysts, modified with Mg(II). Effect of Mg (II) content. Catalysis Today, 213, 50-57.

Dou, B., Wang, C., Song, Y., Chen, H., Xu, Y., 2014. Activity of Ni–Cu–Al based catalyst for renewable hydrogen production from steam reforming of glycerol. Energy Conversion and Management, 78, 253-259.

Ebshish, A., Yaakob, Z., Narayanan, B., Bshish, A., Daud, W.R.W., 2012. Steam Reforming of Glycerol over Ni Supported Alumina Xerogel for Hydrogen Production. Energy Procedia, 19, 552-559.

Escribà, M., Eras, J., Villorbina, G., Balcells, M., Blanch, C., Barniol, N., Canela R., 2011. Use of crude glycerol from biodiesel producers and fatty materials to prepare allyl esters. Waste and Biomass Valorization, 2(3), 285-290.

Franchini, C.A., Aranzaez, W., de Farias, A.M.D., Pecchi, G., Fraga, M.A., 2014. Ce-substituted LaNiO$_3$ mixed oxides as catalyst precursors for glycerol steam reforming. Applied Catalysis B: Environmental, 147, 193-202.

Foo, S.Y., Cheng, C.K., Nguyen, T.H., Kennedy, E.M., Dlugogorski, B.Z., Adesina, A.A., 2012. Carbon deposition and gasification kinetics of used lanthanide-promoted Co-Ni/Al$_2$O$_3$ catalysts from CH$_4$ dry reforming. Catalysis Communications, 2012; 26, 183-188.

Garbarino, G., Wang, C., Valsamakis, I., Chitsazan, S., Riani, P., Finocchio, E., Flytzani-Stephanopoulos, M., Busca, G., 2015., A study of Ni/Al$_2$O$_3$ and Ni–La/Al$_2$O$_3$ catalysts for the steam reforming of ethanol and phenol. Applied Catalysis B: Environmental, 174, 21-34.

Iriondo, A., Barrio, V.L., Cambra, J.F., Arias, P.L., Güemez, M.B., Navarro, R.M., Sanchez-Sanchez M.C., Fierro, J.L.G., 2009. Influence of La_2O_3 modified support and Ni and Pt active phases on glycerol steam reforming to produce hydrogen. Catalysis Communications, 10(8), 1275-1278.

Kachrimanidou, V., Kopsahelis, N., Chatzifragkou, A., Papanikolaou, S., Yanniotis, S., Kookos, I., Koutinas, A.A., 2013. Utilisation of by-products from sunflower-based biodiesel production processes for the production of fermentation feedstock. Waste and Biomass Valorization, 4(3), 529-537.

Khanna, S., Shukla, A.K., Goyal, A., Moholkar, V.S., 2014. Alcoholic biofuels production from biodiesel derived glycerol by clostridium pasteurianum whole cells immobilized on silica. Waste and Biomass Valorization, 5(5), 789-798.

Koo, K.Y., Lee, S.H., Jung, U.H., Roh, H.S. and Yoon, W.L., 2014. Syngas production via combined steam and carbon dioxide reforming of methane over Ni–Ce/$MgAl_2O_4$ catalysts with enhanced coke resistance. Fuel Processing Technology, 119, 151–157.

Manivannan, A., Narendhirakannan, R.T., 2015. Bioethanol production from aquatic weed water fyacinth (eichhornia crassipes) by yeast fermentation. Waste and Biomass Valorization, 6(2), 209-216.

Marx, S., Venter, R. 2014. Evaluation of waste process grease as feedstock for biodiesel production. Waste and Biomass Valorization, 5(1), 75-86.

Mathews, A.P., 2014. Renewable energy technologies: panacea for world energy security and climate change? Procedia Computer Science, 32, 731–737.

Meeyoo, V., Lee, J.H., Trimm, D.L., Cant, N.W., 1998. Hydrogen sulphide emission control by combined adsorption and catalytic combustion. Catalysis Today, 44,67-72.

Melchor-Hernández, C., Gómez-Cortés, A., Díaz, G., 2013., Hydrogen production by steam reforming of ethanol over nickel supported on La-modified alumina catalysts prepared by sol–gel. Fuel, 107, 828-835.

Ngamlerdpokin, K., Kumjadpai, S., Chatanon, P., Tungmanee, U., Chuenchuanchom, S. Jaruwat, P., Lertsathitphongs, P., Hunsom, M., 2011. Remediation of biodiesel wastewater by chemical- and electro-coagulation: A comparative study. Journal of Environmental Management, 92, 2434-2460.

Nuchdang, S., Phalakornkule, C., 2012. Anaerobic digestion of glycerol and co-digestion of glycerol and pig manure. Journal of Environmental Management, 101, 164-172.

Panepinto, D., Viggiano, F., Genon, G., 2014. Evaluation of environmental compatibility for a biomass plant. Waste and Biomass Valorization, 5(5), 759-772.

Passell, H., Dhaliwal H., Reno, M., Wu, B., Amotz, A.B., Ivry, E., Gay, M., Czartoski, T., Laurin, L., Ayer, N., 2013. Algae biodiesel life cycle assessment using current commercial data, Journal of Environmental Management, 129, 103-111.

Pompeo, F., Santori, G.F., Nichio, N.N., 2011. Hydrogen production by glycerol steam reforming with Pt/SiO_2 and Ni/SiO_2 catalysts. Catalysis Today, 172, 183-188.

Pitakpoolsil, W., Hunsom, M., 2014. Treatment of biodiesel wastewater by adsorption with commercial chitosan flakes: Parameter optimaziation and process kinetics. Journal of Environmental Management, 133, 284-292.

Prakash, R., Singh, R.K., Murugan S., 2013. Use of biodiesel and bio-oil emulsions as an alternative fuel for direct injection diesel engine. Waste and Biomass Valorization, 4(3), 475-484.

Qi, Z., He, C., Kaufman, A., 2002. Effect of CO in the anode fuel on the performance of PEM fuel cell cathode. Journal of Power Sources, 111(2), 239-247.

Sánchez-Sánchez, M.C., Navarro, R.M., Fierro, J.L.G., 2007. Ethanol steam reforming over Ni/$_{MxOy}$–$_{Al2O3}$ (M=Ce, La, Zr and Mg) catalysts: Influence of support on the hydrogen production. International Journal of Hydrogen Energy, 32(10-11), 1462-1471.

Siew, K. W., Lee, H.C., Gimbun, J., Cheng, CK., 2014. Production of CO-rich hydrogen gas from glycerol dry reforming over La-promoted Ni/Al$_2$O$_3$catalyst. International Journal of Hydrogen Energy, 39, 6927-6936.

Thyssen, V.V., Maia, T.A., Assaf, E.M., 2013. Ni supported on La$_2$O$_3$–SiO$_2$ used to catalyze glycerol steam reforming. Fuel, 105, 358-363.

Tsipouriari, V.A., Zhang, Z., Verykios, X.E. 1998. Catalytic partial oxidation of methane to synthesis gas over Ni-based catalysts: I. Catalyst performance characteristics. Journal of Catalysis, 179, 283-291.

Winzer, C., 2012. Conceptualizing energy security. Energy Policy, 46, 36-48.

Wu, C., Wang, Z., Wang, L., Huang, J., Williams P.T., 2014. Catalytic steam gasification of biomass for a sustainable hydrogen future: Influence of catalyst composition. Waste and Biomass Valorization, 5(2), 175-180.

Zhang, B., Tang, X., Li, Y., Xu, Y., She, W., 2007. Hydrogen production from steam reforming of ethanol and glycerol over ceria-supported metal catalysts. International Journal of Hydrogen Energy, 32, 2367-2373.